12. Charier, G. *et al.* The tudor tandem of 53BP1: a new structural motif involved in DNA and RG-rich peptide binding. *Structure* **12,** 1551–1562 (2004).
13. Selenko, P. *et al.* SMN tudor domain structure and its interaction with the Sm proteins. *Nature Struct. Biol.* **8,** 27–31 (2001).
14. Sprangers, R., Groves, M. R., Sinning, I. & Sattler, M. High-resolution X-ray and NMR structures of the SMN Tudor domain: conformational variation in the binding site for symmetrically dimethylated arginine residues. *J. Mol. Biol.* **327,** 507–520 (2003).
15. Theobald, D. L., Mitton-Fry, R. M. & Wuttke, D. S. Nucleic acid recognition by OB-fold proteins. *Annu. Rev. Biophys. Biomol. Struct.* **32,** 115–133 (2003).
16. Friesen, W. J., Massenet, S., Paushkin, S., Wyce, A. & Dreyfuss, G. SMN, the product of the spinal muscular atrophy gene, binds preferentially to dimethylarginine-containing protein targets. *Mol. Cell* **7,** 1111–1117 (2001).
17. Brahms, H., Meheus, L., de Brabandere, V., Fischer, U. & Luhrmann, R. Symmetrical dimethylation of arginine residues in spliceosomal Sm protein B/B′ and the Sm-like protein LSm4, and their interaction with the SMN protein. *RNA* **7,** 1531–1542 (2001).
18. Kouzarides, T. Histone methylation in transcriptional control. *Curr. Opin. Genet. Dev.* **12,** 198–209 (2002).
19. Feng, Q. *et al.* Methylation of H3-lysine 79 is mediated by a new family of HMTases without a SET domain. *Curr. Biol.* **12,** 1052–1058 (2002).
20. van Leeuwen, F., Gafken, P. R. & Gottschling, D. E. Dot1p modulates silencing in yeast by methylation of the nucleosome core. *Cell* **109,** 745–756 (2002).
21. Lacoste, N., Utley, R. T., Hunter, J. M., Poirier, G. G. & Cote, J. Disruptor of telomeric silencing-1 is a chromatin-specific histone H3 methyltransferase. *J. Biol. Chem.* **277,** 30421–30424 (2002).
22. Game, J. C., Williamson M. S. & Baccari, C. X-ray survival characteristics and genetic analysis for nine *Saccharomyces* deletion mutants that affect radiation sensitivity. *Genetics* online publication, 15 September 2004 (doi:10.1534/genetics.104.028613).
23. San-Segundo, P. A. & Roeder, G. S. Role for the silencing protein Dot1 in meiotic checkpoint control. *Mol. Biol. Cell* **11,** 3601–3615 (2000).
24. Rogakou, E. P., Boon, C., Redon, C. & Bonner, W. M. Megabase chromatin domains involved in DNA double-strand breaks *in vivo*. *J. Cell Biol.* **146,** 905–916 (1999).
25. Bakkenist, C. J. & Kastan, M. B. DNA damage activates ATM through intermolecular autophosphorylation and dimer dissociation. *Nature* **421,** 499–506 (2003).
26. Celeste, A. *et al.* Histone H2AX phosphorylation is dispensable for the initial recognition of DNA breaks. *Nature Cell Biol.* **5,** 675–679 (2003).
27. Luger, K., Mader, A. W., Richmond, R. K., Sargent, D. F. & Richmond, T. J. Crystal structure of the nucleosome core particle at 2.8 Å resolution. *Nature* **389,** 251–260 (1997).
28. Mozziconacci, J. & Victor, J. M. Nucleosome gaping supports a functional structure for the 30 nm chromatin fiber. *J. Struct. Biol.* **143,** 72–76 (2003).
29. Hyen, Y. *et al.* Structural differences in the DNA binding domains of human p53 and its *C. elegans* ortholog Cep-1. *Structure* **12,** 1237–1243 (2004).
30. Kannouche, P. L., Wing, J. & Lehmann, A. R. Interaction of human DNA polymerase ε with monoubiquitinated PCNA: a possible mechanism for the polymerase switch in response to DNA damage. *Mol. Cell* **14,** 491–500 (2004).

Supplementary Information accompanies the paper on **www.nature.com/nature**.

Acknowledgements The authors thank N. Pavletich, S. Berger, G. Dreyfuss and R. Kaufman for support and discussions, the Wistar Institute Proteomics Facility (K. Speicher) for protein N-terminal sequencing and mass spectrometry analysis, and the University of Pennsylvania Protein Chemistry Facility (J. Lambris and M. Katragadda) for calorimetry analysis. This work was supported by a grant to T.D.H. from the National Cancer Institute.

Competing interests statement The authors declare that they have no competing financial interests.

Correspondence and requests for materials should be addressed to T.D.H. (halazonetis@wistar.upenn.edu). Structure coordinates have been deposited in the Protein Data Bank under the accession code 1XNI.

Structure of a natural guanine-responsive riboswitch complexed with the metabolite hypoxanthine

Robert T. Batey, Sunny D. Gilbert & Rebecca K. Montange

Department of Chemistry and Biochemistry, 215 UCB, University of Colorado, Boulder, Colorado 80309, USA

Riboswitches are genetic regulatory elements found in the 5′ untranslated region of messenger RNA that act in the absence of protein cofactors[1,2]. They are broadly distributed across bacteria and account for the regulation of more than 2% of all genes in *Bacillus subtilis*, underscoring their importance in the control of cellular metabolism[3]. The 5′ untranslated region of many mRNAs of genes involved in purine metabolism and transport contain a guanine-responsive riboswitch that directly binds guanine, hypoxanthine or xanthine to terminate transcription[3,4]. Here we report the crystal structure at 1.95 Å resolution of the purine-binding domain of the guanine riboswitch from the *xpt–pbuX* operon of *B. subtilis* bound to hypoxanthine, a prevalent metabolite in the bacterial purine salvage pathway. This structure reveals a complex RNA fold involving several phylogenetically conserved nucleotides that create a binding pocket that almost completely envelops the ligand. Hypoxanthine functions to stabilize this structure and to promote the formation of a downstream transcriptional terminator element, thereby providing a mechanism for directly repressing gene expression in response to an increase in intracellular concentrations of metabolite.

The remarkable ability of artificially selected RNA 'aptamers' to bind practically any imaginable ligand[5,6] has been harnessed to engineer RNA-based biosensors and molecular machines that respond to environmental cues[7]. These approaches hold considerable promise for real-life applications[8]. Yet, nature has preceded these efforts, as illustrated by naturally occurring RNA sensors, called 'riboswitches', that directly control gene expression through their ability to bind various small-molecule metabolites[1,2]. These sensors are exemplified by the guanine-responsive riboswitch that controls the transcription of genes associated with purine metabolism in numerous bacterial species[3]. The predicted secondary structure of this motif consists of three helices (P1–P3) that surround a three-way junction (Fig. 1a), with phylogenetically conserved nucleotides located in the junction and loops. Immediately downstream of the guanine-binding domain in the mRNA is the switching domain (Fig. 1b), which has been proposed to control gene expression by forming either a terminator or an antiterminator element, depending on whether metabolite is bound[3,4].

To understand how this natural biosensor functions, we have solved by X-ray crystallography the structure of the guanine-binding domain bound to hypoxanthine (Supplementary Table S1 and Supplementary Fig. S1), a biologically relevant ligand of the guanine-responsive riboswitch. In the hypoxanthine-bound state, the RNA adopts a three-dimensional fold in which the terminal loops (L2 and L3) form a series of interconnecting hydrogen bonds (see pairing scheme in Fig. 1a) to bring the P2 and P3 helices parallel to each other (Fig. 1c, d). Unfavourable electrostatic interactions, a result of the juxtaposition of regions of the ribose-phosphate backbone, are neutralized through the binding of several cations between the two backbones (Supplementary Fig. S2). Anchoring the global helical arrangement of the RNA are numerous tertiary contacts around the three-way junction, dominated by the J2/3 loop (Fig. 1c) interacting with bound hypoxanthine, the P1 helix, and the J1/2 and J3/1 loops.

The purine-binding pocket is created by conserved nucleotides in and around the three-way junction element. These nucleotides help to define the purine-binding pocket through the formation of two sets of base triples above and below (Fig. 1a). The 3′ side of the pocket is flanked by a water-mediated U22–A52·A73 base triple and an A23·G46–C53 triple; in both cases, the Watson–Crick face of the adenosine interacts with the minor groove of a Watson–Crick pair (Fig. 2a). The other side is created by sequential base triples between conserved Watson–Crick pairs at the top of helix P1 (U20–A76 and A21–U75) and the Watson–Crick faces of U49 and C50, respectively, which fasten the J2/3 loop to the P1 helix. This extensive use of base triples to create a ligand-binding site is very similar to *in vitro* selected RNA aptamers that recognize planar ring systems, as exemplified by the structures of the theophylline[9], FMN[10] and malachite green[11] binders. Thus, artificially selected RNAs use some of the same principles for creating binding sites for small-molecule ligands as their naturally occurring counterpart.

Hypoxanthine is bound through an extensive series of hydrogen bonds with nucleotides U22, U47, U51 and C74 (Fig. 2b), forming a base quadruple that stacks directly on the P1 helix. The structure clearly shows that the mRNA contacts all of the functional groups in the ligand, thereby explaining the specificity for hypoxanthine observed in biochemical studies[3]. In addition, guanine binding can be readily rationalized, because there is room in the structure to accommodate an exocyclic amine at the 2-position of the bound purine. This additional functional group can form hydrogen bonds with the carbonyl oxygens at the 2-position of C74 and U51, consistent with the tenfold higher affinity of this riboswitch for guanine over hypoxanthine[3].

One of the most marked features is how the ligand is almost completely enveloped by the RNA (Fig. 2c): 97.8% of the surface of hypoxanthine is inaccessible to bulk solvent in the complex. The almost complete use of a ligand for recognition by an RNA is unprecedented among structurally characterized aptamers, although selection strategies that do not involve immobilization of the ligand on a solid support[12] hold promise for the development of RNAs that are capable of a similar degree of ligand burial. This finding also implies that the local binding site must undergo a substantial conformational change upon ligand binding, because it is not possible for hypoxanthine to gain access to a preformed binding site, which is a common feature of many RNA–ligand interactions[13,14]. Finally, this mode of purine recognition also easily explains its ability to change specificity from guanine to adenine

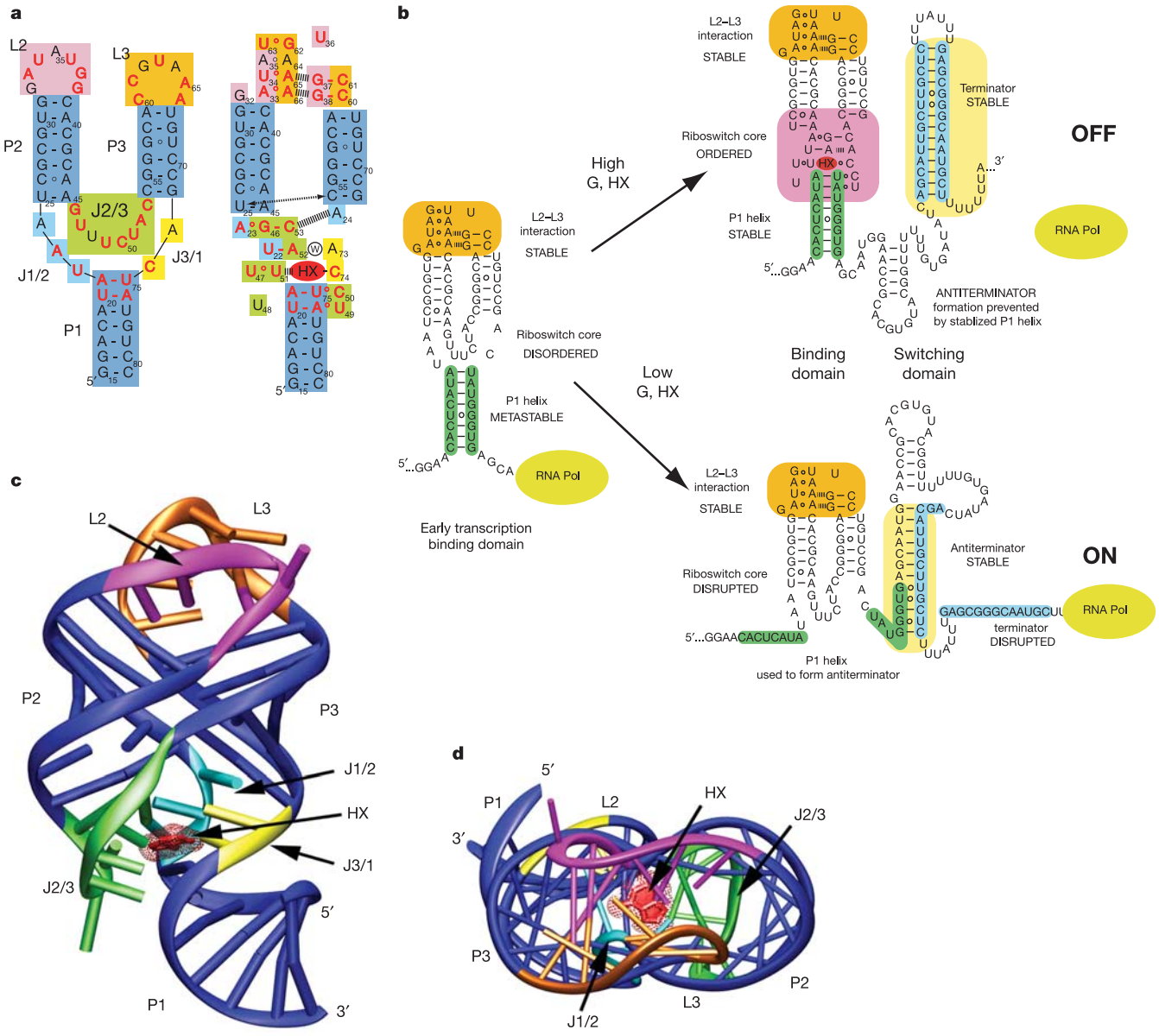

Figure 1 Secondary and tertiary structures of the guanine riboswitch–hypoxanthine complex. **a**, Left, secondary structure of the *xpt–pbuX* guanine-binding domain of the guanine riboswitch of *B. subtilis*[3]. Nucleotides conserved in more than 90% of known guanine riboswitches are shown in red; the numbering is consistent with that of the full-length mRNA. Coloured boxes correspond to structural features shown in Figs 2 and 3. Right, tertiary architecture of the hypoxanthine-bound form. Key tertiary interactions between the loops are shown as thick broken lines; a water-mediated triple is indicated by the circled 'w'. **b**, Gene repression by the guanine riboswitch in the 5′ untranslated region of mRNA. Initial transcription generates a binding domain that is primed to bind guanine (G) rapidly if it is at a sufficiently high concentration. Hypoxanthine (HX, top right) stabilizes the guanine-binding domain and particularly the P1 helix, forcing the mRNA to form a terminator element that halts transcription. In the absence of ligand (bottom right), an antiterminator forms, facilitating continued transcription. **c**, Ribbon representation of the three-dimensional structure of the RNA–hypoxanthine complex. The hypoxanthine ligand is shown in red, with its surface represented by dots. **d**, Top view of the complex, emphasizing the close packing of the P2 and P3 helices.

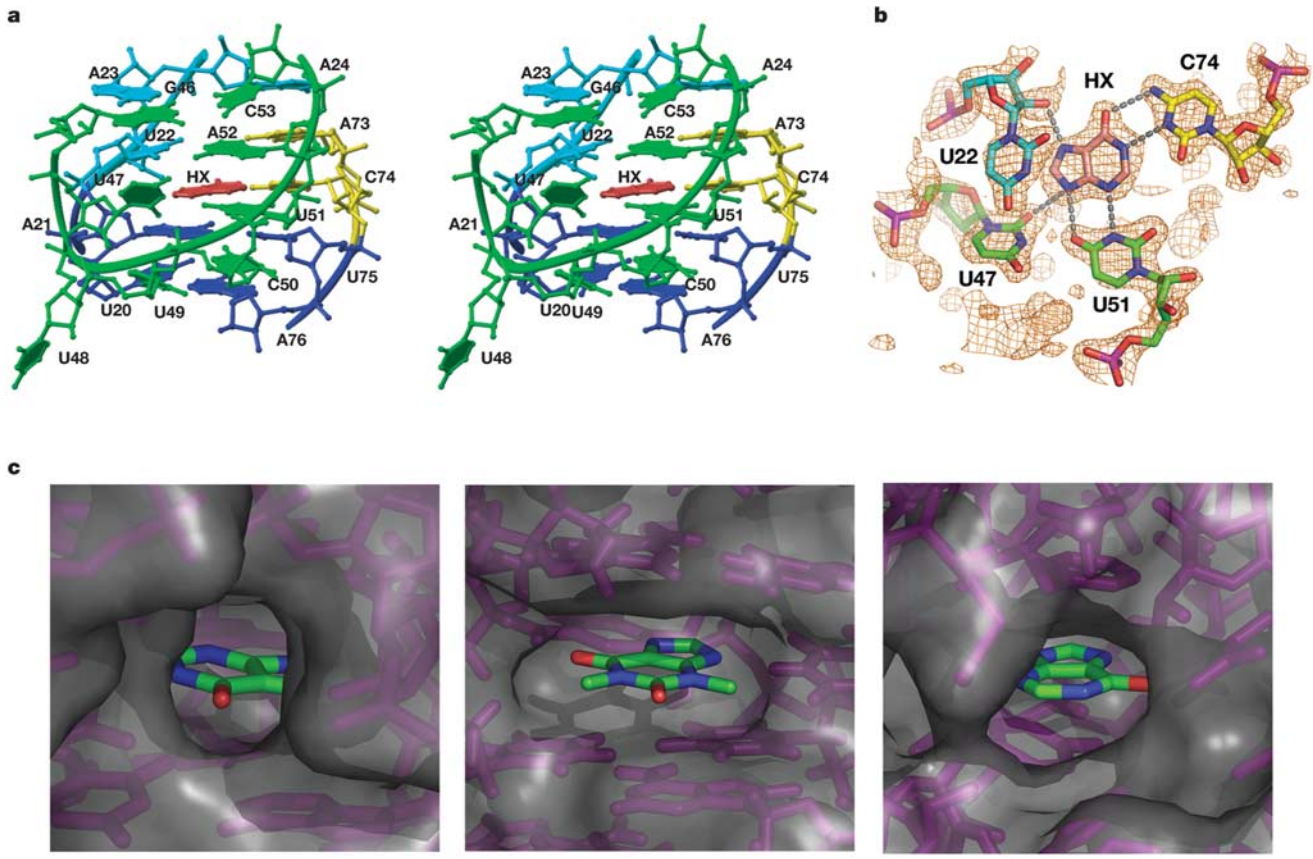

Figure 2 Recognition of hypoxanthine (HX) by the guanine-binding domain. **a**, Stereo view of the hypoxanthine-binding pocket in the three-way junction. **b**, Hydrogen-bonding interactions (grey broken lines) between hypoxanthine and the RNA. The final model (shown in stick representation) is superimposed on a simulated annealing $2F_o–F_c$ omit map (orange cage), in which the atoms shown were excluded from the map calculation. **c**, Molecular surface representation of the binding pocket of the guanine riboswitch bound to hypoxanthine (left), compared with the theophylline-binding aptamer bound to theophylline[9] (centre) and the *E. coli* purR repressor bound to hypoxanthine[28] (right).

through a single point mutation at nucleotide 74 from cytosine to uracil[3,15]. Although the Watson–Crick pairing preference changes from guanine to adenine, the other interactions between the purine and the RNA are unchanged.

The tertiary architecture is stabilized through a unique loop–loop interaction capping helices P2 and P3 that is defined by two previously unobserved types of base quadruple. Each quadruple comprises a Watson–Crick pair with a noncanonical pair docked into its minor groove (G38–C60 and G37–C61 interacting with the A33·A66 and U34·A65 pairs, respectively; Fig. 3a). This arrangement bears a strong similarity to how adenosines pack into an A-form helix in the commonly found type I/II A-minor triple motif[16,17]. Mutation of any one of these eight nucleotides would disrupt the intricate hydrogen-bonding network that cements the core of the loop–loop interaction, explaining their strict phylogenetic conservation. Stacked on these quadruples are two noncanonical pairs, including a side-by-side interaction between G62 and U63 akin to the A-platform motif[18] and the bulged-G motif[19] (Fig. 3b). The G62·U63 pair is further stabilized through hydrogen bonding to the backbone of the opposite loop.

Table 1 **Thermodynamic parameters for hypoxanthine binding at 30 °C**

$MgCl_2$ (mM)	K_d (μM)*	ΔH_{obs} (kcal mol^{-1})*	ΔS_{obs} (cal mol^{-1} K^{-1})
20	0.732 ± 0.034	−33.5 ± 0.43	−82
5.0	1.34 ± 0.094	−28.4 ± 0.48	−67
1.0	2.99 ± 0.19	−35.4 ± 0.93	−91
0.25	4.00 ± 0.19	−41.9 ± 0.39	−113
0†	ND	ND	ND

*The reported errors represent the s.e.m. of the nonlinear least squares fit to the data. ND, no detectable binding.
†This reaction contained 2 mM Na_2-EDTA.

The interaction between the two terminal loops is essential for ligand binding by the guanine riboswitch. Differences in the stability of the RNA in the absence and presence of guanine, as determined by in-line probing experiments[3], indicate that this element of the RNA tertiary structure forms independently of guanine or hypoxanthine. Replacement of the wild-type loops with stable UUCG tetraloops[20] (Supplementary Fig. S3), which eliminates the tertiary interaction, abolishes the ability of the riboswitch to recognize hypoxanthine; this shows that it is crucial for promoting a high-affinity interaction (Fig. 4). Thus, although this tertiary interaction does not contact the ligand directly, it is significant in globally organizing the riboswitch for purine recognition. Similarly, natural sequences of various hammerhead ribozymes contain loop–loop interactions that significantly accelerate their rate of cleavage under physiological conditions[21,22]. In each, the tertiary interaction constrains the RNA in a way that allows the three-way junction containing the functional site to respond to physiological concentrations of ligand or Mg^{2+} ions.

In high Mg^{2+} ion concentrations (20 mM $MgCl_2$), the guanine riboswitch has a very high affinity for guanine and hypoxanthine (an observed dissociation constant (K_d) of 5 nM and 50 nM, respectively)[3]. In *Escherichia coli*, however, repression of transcription of the *xpt–pbuX* operon by the purR repressor occurs in response to 1–10 μM concentrations of purine. To determine whether the riboswitch responds to similar concentrations of purine, which probably reflect physiological levels, we determined its affinity for hypoxanthine by isothermal titration calorimetry at

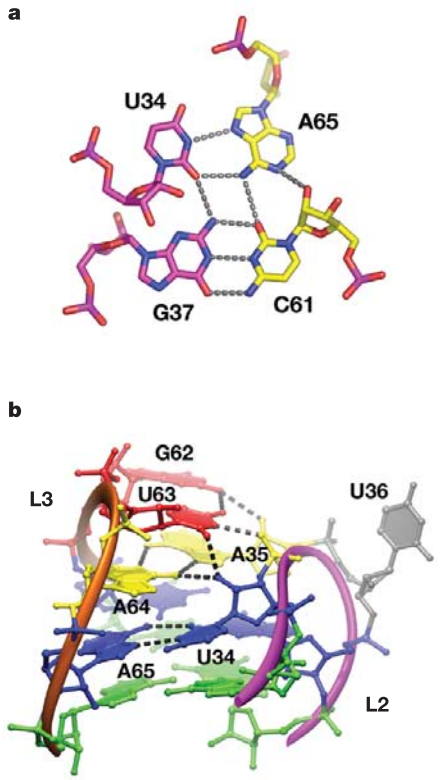

Figure 3 Stabilization of the tertiary architecture. **a**, One of two base quartets that form the core of the loop–loop contact. The carbon atoms are coloured as in Fig. 1. **b**, Side view of the loop–loop interaction, emphasizing the arrangement of base pairs and quartets. The bases of the quartet shown in **a** are coloured blue, with the hydrogen bonding between A65 and U34 shown for orientation; the bases of the other quartet are coloured green. The A35·A64 pair is shown in yellow, with hydrogen bonds emphasizing its interactions with the 2′-hydroxyl group of U34. The capping G62·U63 pair is shown in red.

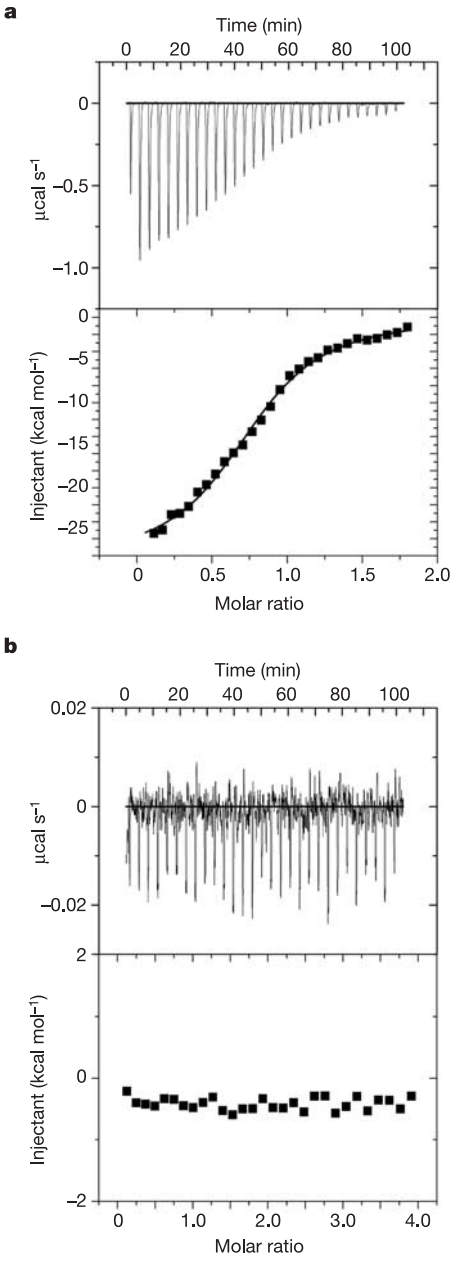

Figure 4 Estimation of the affinity of the riboswitch for hypoxanthine. Shown are the isothermal titration calorimetry curves for the wild-type guanine-binding domain (**a**) and for the guanine-binding domain lacking the tertiary interaction (**b**) with hypoxanthine at 30 °C in buffer containing 10 mM K^+-HEPES (pH 7.5), 100 mM KCl and 5 mM $MgCl_2$.

varying ionic conditions (Table 1). At a more physiological ionic strength (0.25–1 mM Mg^{2+}), the RNA showed an affinity for hypoxanthine (observed $K_d = 3–4\,\mu M$) similar to that of the purR repressor protein (observed $K_d = 9\,\mu M$ for the *E. coli* variant[23]). Thus, both RNA- and protein-based regulatory mechanisms seem to be tuned to respond to similar concentrations of intracellular metabolite. It has been also noted, however, that control of the related adenine riboswitch *in vivo* may be driven in part by the rate of ligand association with the riboswitch, complicating the relationship between intracellular ligand concentration and gene control[4].

The structure further indicates how RNA directly transduces intracellular metabolite concentration into changes in gene expression through a proposed Rho-independent transcriptional regulation mechanism[3,4]. Transcription of the initial ~90 nucleotides results in the formation of the guanine-binding domain, with the L2 and L3 loops interacting to begin to form the tertiary structure of the RNA (Fig. 1b). This partially organizes the three-way junction motif for efficient ligand binding, although the junction must be unstructured to some degree to allow access of the purine to the binding pocket. At sufficiently high concentrations of guanine or hypoxanthine, the nucleobase binds the pocket, stabilizing the short P1 helix through stacking interactions and base triples with J2/3 and preventing incorporation of P1 nucleotides into an antiterminator element. The mRNA can then form a classic Rho-independent terminator stem-loop, and transcription stops. By contrast, in low intracellular concentrations of guanine or hypoxanthine, the 3′ side of the isolated P1 helix is readily conscripted to form a stable antiterminator element, facilitating continued transcription. Thus, hypoxanthine is the keystone for the riboswitch, enabling the riboswitch to direct mRNA folding along two different pathways through its ability to stabilize one conformation over another, resulting in an effective biosensor of intracellular guanine, hypoxanthine and xanthine concentrations. □

Methods

Crystals

We synthesized and purified RNA by a native affinity-tag purification method[24] and exchanged it into a buffer containing 10 mM K^+-HEPES (pH 7.5) and 1 mM hypoxanthine. Crystals were grown by mixing this solution in a 1:1 ratio with mother liquor (containing 25% PEG 3,000 (w/v), 200 mM ammonium acetate and 10 mM cobalt hexamine) and incubating it for 2–3 weeks at room temperature.

Data collection and processing

A single wavelength anomalous diffraction experiment was carried out at the CuKα wavelength on crystals cryoprotected in mother liquor plus 25% 2-methyl-2,4-pentanediol; clear diffraction was observed to at least 1.8 Å resolution. We indexed, integrated and scaled the data using D*TREK[25], identified heavy atom sites with SOLVE[26], and carried out refinement with CNS[27] to obtain a model with final R_{xtal} and R_{free} values of 17.8% and 22.8%, respectively. The model contains all RNA atoms except A82, for which electron density was not observed, along with the hypoxanthine ligand. For additional experimental details and references, see Supplementary Information.

Received 28 July; accepted 13 September 2004; doi:10.1038/nature03037.

1. Vitreschak, A. G., Rodionov, D. A., Mironov, A. A. & Gelfand, M. S. Riboswitches: the oldest mechanism for the regulation of gene expression? *Trends Genet.* **20,** 44–50 (2004).
2. Mandal, M. & Breaker, R. R. Gene regulation by riboswitches. *Nature Rev. Mol. Cell. Biol.* **5,** 451–463 (2004).
3. Mandal, M., Boese, B., Barrick, J. E., Winkler, W. C. & Breaker, R. R. Riboswitches control fundamental biochemical pathways in *Bacillus subtilis* and other bacteria. *Cell* **113,** 577–586 (2003).
4. Johansen, L. E., Nygaard, P., Lassen, C., Agerso, Y. & Saxild, H. H. Definition of a second *Bacillus subtilis pur* regulon comprising the *pur* and *xpt–pbuX* operons plus *pbuG*, *nupG* (*yxjA*), and *pbuE* (*ydhL*). *J. Bacteriol.* **185,** 5200–5209 (2003).
5. Ellington, A. D. & Szostak, J. W. *In vitro* selection of RNA molecules that bind specific ligands. *Nature* **346,** 818–822 (1990).
6. Gold, L., Polisky, B., Uhlenbeck, O. & Yarus, M. Diversity of oligonucleotide functions. *Annu. Rev. Biochem.* **64,** 763–797 (1995).
7. Silverman, S. K. Rube Goldberg goes (ribo)nuclear? Molecular switches and sensors made from RNA. *RNA* **9,** 377–383 (2003).
8. Seetharaman, S., Zivarts, M., Sudarsan, N. & Breaker, R. R. Immobilized RNA switches for the analysis of complex chemical and biological mixtures. *Nature Biotechnol.* **19,** 336–341 (2001).
9. Zimmermann, G. R., Jenison, R. D., Wick, C. L., Simmorre, J.-P. & Pardi, A. Interlocking structural motifs mediate molecular discrimination by a theophylline-binding RNA. *Nature Struct. Biol.* **4,** 644–649 (1997).
10. Fan, P., Suri, A. K., Fiala, R., Live, D. & Patel, D. J. Molecular recognition in the FMN–RNA aptamer complex. *J. Mol. Biol.* **258,** 480–500 (1996).
11. Baugh, C., Grate, D. & Wilson, C. 2.8 Å crystal structure of the malachite green aptamer. *J. Mol. Biol.* **301,** 117–128 (2000).
12. Koizumi, M., Soukup, G. A., Kerr, J. N. & Breaker, R. R. Allosteric selection of ribozymes that respond to the second messengers cGMP and cAMP. *Nature Struct. Biol.* **6,** 1062–1071 (1999).
13. Leulliot, N. & Varani, G. Current topics in RNA–protein recognition: control of specificity and biological function through induced fit and conformational capture. *Biochemistry* **40,** 7947–7956 (2001).
14. Williamson, J. R. Induced fit in RNA–protein recognition. *Nature Struct. Biol.* **7,** 834–837 (2000).
15. Mandal, M. & Breaker, R. R. Adenine riboswitches and gene activation by disruption of a transcription terminator. *Nature Struct. Mol. Biol.* **11,** 29–35 (2004).
16. Doherty, E. A., Batey, R. T., Masquida, B. & Doudna, J. A. A universal mode of helix packing in RNA. *Nature Struct. Biol.* **8,** 339–343 (2001).
17. Nissen, P., Ippolito, J. A., Ban, N., Moore, P. B. & Steitz, T. A. RNA tertiary interactions in the large ribosomal subunit: the A-minor motif. *Proc. Natl Acad. Sci. USA* **98,** 4899–4903 (2001).
18. Cate, J. H. *et al.* RNA tertiary structure mediation by adenosine platforms. *Science* **273,** 1696–1699 (1996).
19. Correll, C. C., Beneken, J., Plantinga, M. J., Lubbers, M. & Chan, Y. L. The common and the distinctive features of the bulged-G motif based on a 1.04 Å resolution RNA structure. *Nucleic Acids Res.* **31,** 6806–6818 (2003).
20. Molinaro, M. & Tinoco, I. Jr Use of ultra stable UNCG tetraloop hairpins to fold RNA structures: thermodynamic and spectroscopic applications. *Nucleic Acids Res.* **23,** 3056–3063 (1995).
21. De la Pena, M., Gago, S. & Flores, R. Peripheral regions of natural hammerhead ribozymes greatly increase their self-cleavage activity. *EMBO J.* **22,** 5561–5570 (2003).
22. Khvorova, A., Lescoute, A., Westhof, E. & Jayasena, S. D. Sequence elements outside the hammerhead ribozyme catalytic core enable intracellular activity. *Nature Struct. Biol.* **10,** 708–712 (2003).
23. Choi, K. Y. & Zalkin, H. Structural characterization and corepressor binding of the *Escherichia coli* purine repressor. *J. Bacteriol.* **174,** 6207–6214 (1992).
24. Kieft, J. S. & Batey, R. T. A general method for rapid and nondenaturing purification of RNAs. *RNA* **10,** 988–995 (2004).
25. Pflugrath, J. W. The finer things in X-ray diffraction data collection. *Acta Crystallogr. D* **55,** 1718–1725 (1999).
26. Terwilliger, T. SOLVE and RESOLVE: automated structure solution, density modification and model building. *J. Synchrotron Radiat.* **11,** 49–52 (2004).
27. Brunger, A. T. *et al.* Crystallography & NMR system: a new software suite for macromolecular structure determination. *Acta Crystallogr. D* **54,** 905–921 (1998).
28. Schumacher, M. A., Choi, K. Y., Zalkin, H. & Brennan, R. G. Crystal structure of LacI member, PurR, bound to DNA: minor groove binding by α helices. *Science* **266,** 763–770 (1994).

Supplementary Information accompanies the paper on **www.nature.com/nature**.

Acknowledgements We thank S. Edwards for maintaining and managing the Biochemistry Division X-ray Crystallography facility; and T. Cech, A. Pardi, D. Wuttke, J. Kieft and R. Rambo for discussions and comments on the manuscript. This work was funded in part from a grant from the Research Corporation and the University of Colorado Butcher Biotechnology Initiative. S.D.G. was supported in part by a NIH predoctoral training grant.

Competing interests statement The authors declare that they have no competing financial interests.

Correspondence and requests for materials should be addressed to R.T.B. (robert.batey@colorado.edu). The atomic coordinates and structure factors have been deposited in the RCSB Protein Data Bank under accession number 1U8D.

corrigendum

The genome of *Cryptosporidium hominis*

Ping Xu, Giovanni Widmer, Yingping Wang, Luiz S. Ozaki, Joao M. Alves, Myrna G. Serrano, Daniela Puiu, Patricio Manque, Donna Akiyoshi, Aaron J. Mackey, William R. Pearson, Paul H. Dear, Alan T. Bankier, Darrell L. Peterson, Mitchell S. Abrahamsen, Vivek Kapur, Saul Tzipori & Gregory A. Buck

Nature **431,** 1107–1112 (2004).

The GenBank accession number was supplied incorrectly as AAEL000000. The sentence should have read: 'The sequences reported in this paper have been deposited in GenBank under the project accession number AAEL00000000.'. In addition, the received date should have been 14 March 2004. □